archaea are about 8.7‰ versus AIR (Table 1), or 6.2‰ versus supplied NH_4^+. These values are much higher than for AOB and are in line with $\delta^{15}N_{N2O}$ values reported for the shallow subsurface source of N_2O in the North Pacific (*8*) and the global ocean (*24*, *26*), assuming a reduced organic N source similar to suspended particulate nitrogen [–1 to 5‰; (*27*)]. $\delta^{18}O_{N2O}$ values also fall within the range necessary to close the global N_2O budget and supply the subsurface source of N_2O to the North Pacific (*8*). Site preferences measured here for AOA, however, are higher than modeled in situ production values (SP = –0.6 to 7.2‰) estimated by (*8*). This suggests that N_2O production by AOA in situ may be associated with low-oxygen microenvironments producing more N_2O by NO_2^- reduction with a lower mean site preference than measured in aerobic batch culture.

With the demonstration of high abundances of AOA coincident with high nitrification rates (*15*, *28*), and now the ability of AOA to produce N_2O with the appropriate isotopic signatures, we suggest that AOA likely play an important role in N_2O production in the near-surface ocean.

References and Notes

1. S. Solomon, *Climate Change 2007: The Physical Science Basis* (Cambridge Univ. Press, Cambridge, 2007).
2. C. Nevison, T. Lueker, R. Weiss, *Global Biogeochem. Cycles* **18**, GB1018 (2004).
3. N. E. Ostrom, M. E. Russ, B. N. Popp, T. M. Rust, D. M. Karl, *Chemosphere, Glob. Chang. Sci.* **2**, 281 (2000).
4. L. Codispoti, J. Christensen, *Mar. Chem.* **16**, 277 (1985).
5. J. W. Elkins, S. C. Wofsy, M. B. McElroy, C. E. Kolb, W. A. Kaplan, *Nature* **275**, 602 (1978).
6. K. R. Kim, H. Craig, *Nature* **347**, 58 (1990).
7. J. E. Dore, B. N. Popp, D. M. Karl, F. J. Sansone, *Nature* **396**, 63 (1998).
8. B. N. Popp *et al.*, *Global Biogeochem. Cycles* **16**, 1064 (2002).
9. S. Naqvi *et al.*, *Nature* **394**, 462 (1998).
10. N. Yoshida, *Nature* **335**, 528 (1988).
11. M. B. Karner, E. F. DeLong, D. M. Karl, *Nature* **409**, 507 (2001).
12. M. Könneke *et al.*, *Nature* **437**, 543 (2005).
13. C. Wuchter *et al.*, *Proc. Natl. Acad. Sci. U.S.A.* **103**, 12317 (2006).
14. W. Martens-Habbena, P. M. Berube, H. Urakawa, J. R. de la Torre, D. A. Stahl, *Nature* **461**, 976 (2009).
15. A. E. Santoro, K. L. Casciotti, C. A. Francis, *Environ. Microbiol.* **12**, 1989 (2010).
16. A. E. Santoro, K. L. Casciotti, *ISME J.* (2011); doi:10.1038/ismej.2011.58.
17. Materials and methods are available as supporting material on *Science* Online.
18. T. J. Goreau *et al.*, *Appl. Environ. Microbiol.* **40**, 526 (1980).
19. C. Frame, K. Casciotti, *Biogeosciences* **7**, 2695 (2010).
20. N. Yoshida, S. Toyoda, *Nature* **405**, 330 (2000).
21. R. D. Dua, B. Bhandari, D. J. Nicholas, *FEBS Lett.* **106**, 401 (1979).
22. K. Andersson, A. Hooper, *FEBS Lett.* **164**, 236 (1983).
23. K. L. Casciotti, M. R. McIlvin, C. Buchwald, *Limnol. Oceanogr.* **55**, 753 (2010).
24. K. R. Kim, H. Craig, *Science* **262**, 1855 (1993).
25. K. L. Casciotti, D. M. Sigman, M. G. Hastings, J. K. Böhlke, A. Hilkert, *Anal. Chem.* **74**, 4905 (2002).
26. T. Rahn, M. Wahlen, *Global Biogeochem. Cycles* **14**, 537 (2000).
27. J. E. Dore, J. R. Brum, L. M. Tupas, D. M. Karl, *Limnol. Oceanogr.* **47**, 1595 (2002).
28. J. M. Beman, B. N. Popp, C. A. Francis, *ISME J.* **2**, 429 (2008).

Acknowledgments: We thank C. Wuchter, S. Sievert, and M. Johnson for assistance in the laboratory. We also thank C. Frame, L. Codispoti, and three anonymous reviewers for helpful discussions and feedback. Funding for this work was provided by the Woods Hole Oceanographic Institution Ocean Life Institute, a Woods Hole Oceanographic Institution Postdoctoral Scholar Fellowship to A.E.S., and U.S. National Science Foundation grants OCE-0526277 and OCE-0961098 to K.L.C. The 16*S* ribosomal RNA gene and *amoA* gene sequences for CN25 and CN75 have been deposited in GenBank under the accession nos. HQ338108, JF521547, and JF521548. The CN25 and CN75 strains are available by request from A.E.S.

Supporting Online Material

www.sciencemag.org/cgi/content/full/1208239/science.DC1
Materials and Methods
Fig. S1
Table S1
References (*29*–*47*)

11 May 2011; accepted 13 July 2011
Published online 28 July 2011;
10.1126/science.1208239

Out of Tibet: Pliocene Woolly Rhino Suggests High-Plateau Origin of Ice Age Megaherbivores

Tao Deng,[1] Xiaoming Wang,[1,2]* Mikael Fortelius,[1,3] Qiang Li,[1] Yang Wang,[4] Zhijie J. Tseng,[2,5] Gary T. Takeuchi,[6] Joel E. Saylor,[7] Laura K. Säilä,[3] Guangpu Xie[8]

Ice Age megafauna have long been known to be associated with global cooling during the Pleistocene, and their adaptations to cold environments, such as large body size, long hair, and snow-sweeping structures, are best exemplified by the woolly mammoths and woolly rhinos. These traits were assumed to have evolved as a response to the ice sheet expansion. We report a new Pliocene mammal assemblage from a high-altitude basin in the western Himalayas, including a primitive woolly rhino. These new Tibetan fossils suggest that some megaherbivores first evolved in Tibet before the beginning of the Ice Age. The cold winters in high Tibet served as a habituation ground for the megaherbivores, which became preadapted for the Ice Age, successfully expanding to the Eurasian mammoth steppe.

Among the most iconic Ice Age mammals, the woolly rhino (*Coelodonta*) was widespread in northern Eurasia and adapted to cold climates in the mammoth steppe during the late Pleistocene (*1*–*3*). The known fossil record suggests that the woolly rhino evolved in Asia, but its early ancestry remains elusive (*3*–*6*). Our new middle Pliocene (~3.7 million years ago) woolly rhino, *Coelodonta thibetana* sp. nov., from the high-altitude Zanda Basin in the foothills of the Himalayas in southwestern Tibet, occupies the most basal position of the *Coelodonta* lineage and is the earliest representative of the genus. As the Ice Age began about 2.8 million years ago, the Tibetan woolly rhino descended, through intermediate forms, to low-altitude, high-latitude regions in northern Eurasia, and along with the Tibetan yak, argali, and bharal, became part of the emerging *Mammuthus-Coelodonta* fauna in the middle to late Pleistocene.

Coelodonta thibetana is described as follows: Perissodactyla Owen, 1848. Rhinocerotidae Owen, 1845. *Coelodonta* Bronn, 1831. ***Coelodonta thibetana*** sp. nov. **Holotype**. A complete skull and mandible with associated atlas, axis, and third cervical vertebra, representing a full adult individual, Institute of Vertebrate Paleontology and Paleoanthropology (IVPP), Beijing, China, specimen no. V15908 (Fig. 1A); discovered by X.W. on 22 August 2007 and collected by a field team led by G.T.T. **Etymology**. The specific name, *thibetana*, refers to the geographical location of the discovery. **Type locality and horizon**. IVPP locality ZD0740 (31°33'55.3"N, 79°50'53.8"E, elevation 4207 m) is 10.2 km northeast of the Zanda county seat, Ngari District, Tibet Autonomous Region, China (fig. S2). IVPP V15908 is from the upper part of the middle fine-grained sequence in the upper Zanda Formation [see supporting online material (SOM) for details].

[1]Key Laboratory of Evolutionary Systematics of Vertebrates, Institute of Vertebrate Paleontology and Paleoanthropology, Chinese Academy of Sciences, Beijing 100044, China. [2]Department of Vertebrate Paleontology, Natural History Museum of Los Angeles County, Los Angeles, CA 90007, USA. [3]Department of Geosciences and Geography, FIN-00014 University of Helsinki, Helsinki, Finland. [4]Department of Earth, Ocean and Atmospheric Science, Florida State University, and National High Magnetic Field Laboratory, Tallahassee, FL 32306, USA. [5]Integrative and Evolutionary Biology Program, Department of Biological Sciences, University of Southern California, Los Angeles, CA 90089, USA. [6]The George C. Page Museum, 5801 Wilshire Boulevard, Los Angeles, CA 90036, USA. [7]Department of Geological Sciences, Jackson School of Geosciences, University of Texas at Austin, Austin, TX 78712, USA. [8]Gansu Provincial Museum, Lanzhou 730050, China.

*To whom correspondence should be addressed. E-mail: xwang@nhm.org

Age. IVPP locality ZD0740 is faunally and paleomagnetically dated to the top of chron C2Ar with an estimated age of 3.7 million years ago (Ma) in the middle Pliocene (fig. S3).

Diagnosis. *Coelodonta thibetana* possesses typical characteristics of the genus, such as a dolichocephalic skull, an ossified nasal septum, an enlarged mediolaterally compressed nasal horn boss with a longitudinal crest, nasals bent downward anteriorly, occipital crest elevated and posteriorly extended, high tooth crowns with rough enamel and coronal cement, and visible medi- and post-fossettes at an early stage of wear. It differs from other, more derived species of woolly rhinos (*C. nihowanensis*, *C. tologoijensis*, and *C. antiquitatis*) in having a less well-developed nasal septum, which is only one-third of the length of the nasal notch; a more anteriorly positioned mandibular symphysis; less-derived molar morphology with thinner coronal cement; a less wavy ectoloph profile with a less prominent mesostyle on M2; a triangular occlusal outline of M3; a blunt anterior edge of the paraconid and a sigmoidal hypolophid with a distinctly recurved posterior end; and weak anterior ribs on m2-3.

Description and comparison (Fig. 1A). The skull of *Coelodonta thibetana* is highly dolichocephalic (width/length ratio = 0.39) (Fig. 1A), with a relatively long face as is characteristic of the genus. As in *C. nihowanensis* (*7*) and *C. antiquitatis* (*8*), the nasal horn boss is strongly roughened and relatively large, occupying the entire dorsal surface of the nasal, indicating a large nasal horn. A wide and low dome on the frontals indicates the presence of a smaller frontal horn. The relative size of the nasal horn is greater than in extant and fossil rhinocerotines, resembling those of elasmotheres or dicerotines, but narrower in shape. As is typical of rhinoceroses with a low-slung head position for feeding at ground level (*9*), the occipital surface is reclined posteriorly, and the occipital crest is straight and backward, overhanging the occipital condyle to a similar extent as in *C. nihowanensis* and less than in more-derived woolly rhinos (see additional description and comparison in SOM).

Phylogeny. Our phylogenetic analysis of 5 extant and 13 extinct Rhinoceratini taxa places *C. thibetana* as a derived dicerorhine, nested within a clade of Mio-Pleistocene species of *Stephanorhinus* (Fig. 2A). The larger and heavier species such as *Dihoplus ringstroemi, D. megarhinus* (*10*), and *"D." kirchbergensis* consistently appear outside a clade including the more lightly built forms of *Stephanorhinus* (*S. etruscus*, *S. hundsheimensis*, and *S. hemitoechus*) as well as *Coelodonta*. In all of the most parsimonious trees, the sister taxon of the *Coelodonta* clade is *S. hemitoechus* (Fig. 2A), a middle-to-late Pleistocene species. Within the *Coelodonta* clade, our phylogenetic analysis produced a series of progressively more-derived species from *C. thibetana*, through *C. nihowanensis* and *C. tologoijensis*, and terminating in *C. antiquitatis* (Fig. 2A) (see SOM for details of the analysis).

We analyzed the carbon and oxygen isotopic compositions of fossil horses, rhinos, deer, and

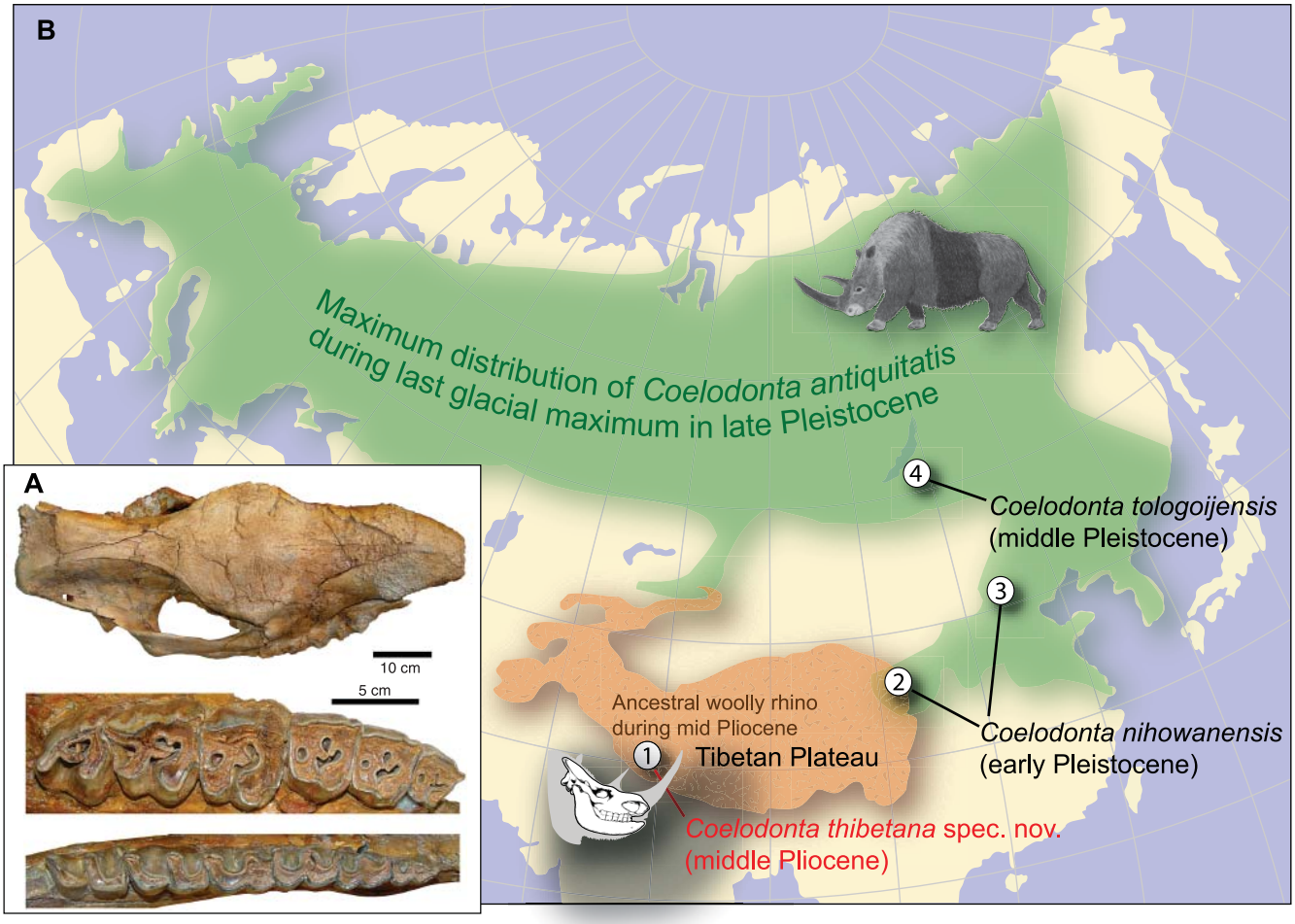

Fig. 1. (**A**) Dorsal view of the skull (upper), occlusal view of upper cheek teeth (middle), and occlusal view of lower cheek teeth (lower) of the new woolly rhino *C. thibetana* sp. nov. (IVPP V15908). (**B**) Origin, distribution, and dispersal of woolly rhinos in Eurasia, simplified from Kahlke and Lacombat (*3*). The late Pleistocene distribution of *C. antiquitatis* is shown in green; the distribution of other *Coelodonta* species is shown by the circled numbers. [The life reconstruction of a woolly rhino is by L.K.S.; the reconstruction of the skull and mandible of *C. thibetana* is by Shen Wenlong]

bovids from Zanda Basin as well as modern Tibetan wild asses (*Equus kiang*) (see SOM for details). The enamel $\delta^{13}C$ values for the time period of 3.1 to 4.0 Ma are –9.6 ± 0.8 per mil (‰) (n = 110 samples), indicating that these ancient herbivores, just like modern Tibetan asses in the area, primarily fed on C_3 vegetation and lived in an environment dominated by C_3 plants (Fig. 2, B and C). The enamel $\delta^{18}O$ values of mid-Pliocene obligate drinkers (i.e., the horse and rhino) are lower than those of their modern counterpart, probably indicating a shift in climate to much drier conditions after ~3 to 4 Ma (Fig. 2, B and C). Using the $\delta^{18}O$ values of fossil gastropods, Saylor *et al.* (*11*) estimated that the paleoelevation for the Mio-Pliocene Zanda Basin was at least as high as and possibly up to 1.5 km higher than today. This high elevation estimate is consistent with a cold (similar to modern) climate with lengthy subfreezing temperatures during the winters.

As in the woolly mammoth and the modern Tibetan yaks, the presence of long woolly fur for thermal insulation in *Coelodonta antiquitatis* (a descendant of *C. thibetana*) strongly suggests that it was adapted to life in the cold tundra and steppe. In addition to using thick wool and increased body size to conserve heat, the cranial and horn complex in all woolly rhinos is also well integrated for cold conditions. Although the classic notion that the long, forward-leaning, and bilaterally flattened horn of the woolly rhino was used to plough through icy snow in order to feed during the winter (*12*) is untenable for multiple reasons, the possibility that the horn was used to expose ground vegetation by sweeping loose snow is entirely plausible (*3*, *13*). Several morphological features are in favor of such an interpretation: (i) The horn of the woolly rhino tends to be more forwardly inclined (seen in preserved Ice Age cave paintings), usually to the point that the top portion of the horn is in front of the nose tip; (ii) there is frequently an anterior wear facet along the leading edge of the horn; (iii) this facet is usually keeled, consisting of a right and left wear facet, presumably produced by a sweeping motion of the tilted head as the horn swept over snowy vegetation; (iv) the bilateral flattening (anteroposterior elongation) of the horn, in contrast to the mostly rounded cross section in most living rhinos, gives the woolly rhino added profile for increased effective sweeping area; (v) there is a posteriorly reclined skull (occiput), which would assist in lowering of the head. These cranial features, in combination with long and woolly hair, are strong indications of a species adapted for survival in cold, snow-covered terrains.

The skull of the Zanda woolly rhino shows signs of the snow-sweeping morphologies. A large nasal horn boss indicates a differentially enlarged nasal horn relative to the frontal horn.

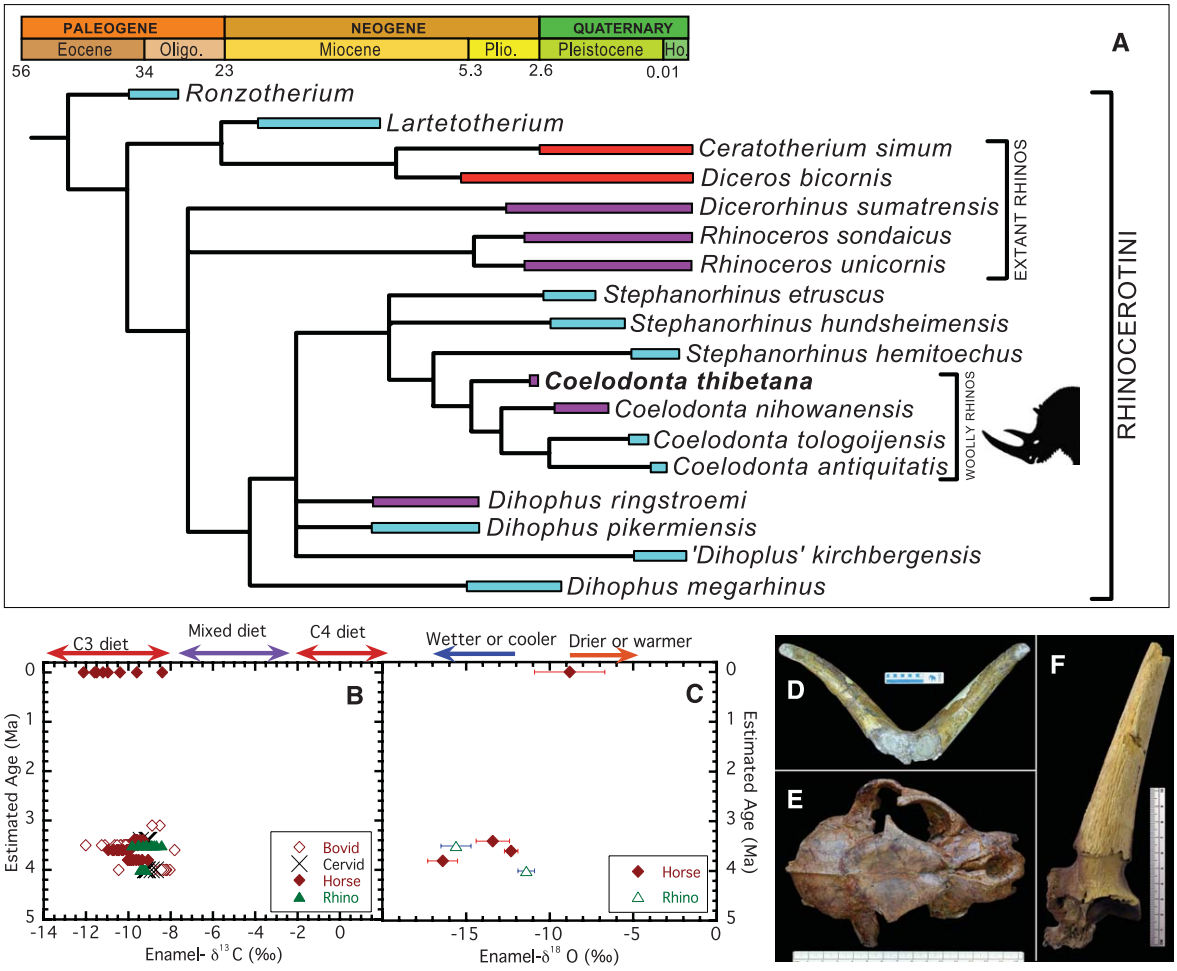

Fig. 2. (**A**) Phylogenetic position of *C. thibetana* within the Rhinocerotini. A strict consensus cladogram of nine most parsimonious trees plotted against geological time is shown, with colored boxes representing the known time period of each species. The color of the box indicates geographical distribution as follows: red, Africa; blue, Eurasia; purple, Far East (including East Asia and Southeast Asia). We analyzed a modified subset of characters and taxa from Antoine (*24*); see SOM for additional details. (**B**) $\delta^{13}C$ values of bulk and serial enamel samples from herbivores and (**C**) the mean enamel $\delta^{18}O$ values of obligate drinkers in the Zanda Basin. (**D** to **F**) Three large mammals from the Zanda fauna: (D) posterior view of the horn core of a blue sheep ?*Pseudois* sp. from ZD0712 (~3.5 Ma); scale = 10 cm; (E) dorsal view of the skull of a primitive snow leopard [*Panthera* (*Uncia*) sp.] from ZD1001 (~4.4 Ma); scale is in millimeters; (F) anterior view of the horn core of an ancestral Tibetan antelope, *Qurliqnoria* from ZD0745 (~4.2 Ma); scale is in millimeters. See also Table 1 for zoogeographic scenarios.

Table 1. Stepping down: Paleogeographic scenarios of several Tibetan mammals (see SOM for detailed documentation).

Species	Ancestry	Zoogeographic scenarios	Present distribution
Woolly rhino (*C. thibetana*)	Tibet	Through transitional species along edge of Tibet and central Asia, expanding to entire northern Eurasia	Extinct
Tibetan wild yak (*Bos mutus*)	Tibet?	Sister to European and North American bison	Tibetan Plateau only
Tibetan wild ass (*Equus kiang*)	?	Pleistocene expansion to northern Pakistan and possibly Alaska	Tibetan Plateau only
Argali (*Ovis ammon*)	?	Pleistocene expansion to northern Eurasia, gave rise to snow sheep in Siberia, which in turn gave rise to North American bighorns	Tibetan Plateau and surrounding regions
Chiru (Tibetan antelope) (*Pantholops hodgsonii*)	Tibet	Originated in northern Tibetan Plateau during late Miocene as *Qurliqnoria*, which gave rise to *Pantholops*	Tibetan Plateau only
Tibetan bharal (blue sheep) (*Pseudois nayaur*)	Tibet	Primitive form in Pliocene of Tibet and expanding to north and northeast China during Pleistocene	Tibetan Plateau only
Snow leopard [*Panthera* (*Uncia*) *uncia*]	Tibet	Primitive form in Pliocene of Tibet and expanding to surrounding regions during Pleistocene	Tibetan Plateau and surrounding regions

This attachment area of the nasal horn shows a weak central bump, proximally and distally flanked by a weakly developed version of the central crest that characterizes this anatomical region in the Pleistocene species. This arrangement indicates that the nasal horn was already bilaterally flattened at least to some degree. Furthermore, the downwardly curved nasal tip indicates a strongly forwardly inclined horn, and the posteriorly reclined occiput indicates a habitually low-slung cranial posture for feeding at ground level. Collectively, these cranial features lend support for snow-clearing adaptations, which became a key preadaptation for its Pleistocene descendants.

The last representatives of the woolly rhino disappeared at the end of the Pleistocene, about 0.01 Ma (*14*). In addition to this new species from Tibet, only three species are commonly recognized (*15*): *C. nihowanensis* from the early Pleistocene (about 2.5 Ma) of northern China (*6*), *C. tologoijensis* from the middle Pleistocene (about 0.75 Ma) of the Lake Baikal area of eastern Siberia to the middle Pleistocene of western Europe (*3*, *16*), and *C. antiquitatis* from the late Pleistocene of northern Eurasia (*3*, *8*). All known species of the woolly rhino lived in cold conditions in northern Eurasia, especially Siberia (*15*, *16*), and a few rare southern forms are from high-elevation regions, such as Aba (*17*), Gonghe (*18*), and Linxia (*6*), in or along the eastern margin of the Tibetan Plateau. Such a striking zoogeographic pattern of progressive expansion from Tibet, coupled with the congruence of phylogeny and chronology, suggests a scenario in which ancestral woolly rhinos from high-altitude Tibet descended to high-latitude Siberia (Fig. 1B). As global climate cooled and cold habitats expanded, the ancestral woolly rhino descended to northern latitudes and, eventually turning to grazing in the late Pleistocene (*3*), became one of the most successful Ice Age megaherbivores.

The woolly rhino is probably not the only case of a Tibetan cold-adapted ancestor to give rise to Ice Age megafauna. A composite Zanda fauna (Table 1 and table S1), as well as Mio-Pliocene records from elsewhere in the plateau (*19*), suggests that a distinct Tibetan fauna was in place going back as far as the late Miocene. A progenitor of the Tibetan bharal (*Pseudois nayaur*) appeared in the Zanda Basin and expanded to northern Asia during the Ice Age (SOM), a very similar history to that of the woolly rhino. Furthermore, molecular phylogenies for the Tibetan yak (*Bos mutus*) and central Asian argali (*Ovis ammon*) suggest links between presumed Tibetan (or surrounding mountains) ancestors and their North American megafauna relatives, such as the bison (*Bison bison*) and bighorn sheep (*Ovis canadensis*) (*20*, *21*). Woolly rhino–like in its large size and woolly hair, the Tibetan yak has been recognized as far north as the Lake Baikal area during the Pleistocene (*22*). Thus, although the origin of the cold-adapted Pleistocene megafauna has usually been sought either in the circumpolar tundra or in the cool steppes of the Pliocene and early Pleistocene (*15*, *23*), the harsh winters of the rising Tibetan Plateau could well have provided the initial step toward cold adaptation for several subsequently successful members of the late Pleistocene mammoth fauna of the Holarctic.

References and Notes

1. C. Guérin, *Cranium* **2**, 3 (1989).
2. D. R. Prothero, C. Guérin, E. Manning, in *The Evolution of Perissodactyls,* D. R. Prothero, R. M. Schoch, Eds. (Oxford Univ. Press, New York, 1989), pp. 321–340.
3. R.-D. Kahlke, F. Lacombat, *Quat. Sci. Rev.* **27**, 1951 (2008).
4. T. Deng, *Cour. Forsch.-Inst. Senckenberg* **256**, 43 (2006).
5. L. Orlando *et al*., *Mol. Phylogenet. Evol.* **28**, 485 (2003).
6. Z.-x. Qiu, T. Deng, B. Y. Wang, *Palaeontol. Sinica N.S.C* **27**, 1 (2004).
7. T. Deng, *Geol. Bull. China* **21**, 604 (2002).
8. J. C. Zachos, G. R. Dickens, R. E. Zeebe, *Nature* **451**, 279 (2008).
9. F. E. Zeuner, *Ber. Naturf. Ges. Freiburg.* **34**, 21 (1934).
10. I. X. Giaourtsakis, *Beitr. Paläont.* **31**, 157 (2009).
11. J. E. Saylor *et al*., *Am. J. Sci.* **309**, 1 (2009).
12. E. Haase, *Tiere der Verzeit* (Verlag von Quelle & Meyer, Leipzig, Germany, 1914).
13. M. Fortelius, *J. Vertebr. Paleontol.* **3**, 125 (1983).
14. N. Thew, L. Chaix, C. Guérin, in *La Faune*, D. Aubry, M. Guélat, J. Detrey, B. Othenin-Girard, Eds. (Cahier d'Archéologie Jurassienne, Porrentruy, Switzerland, 2000), pp. 93–98.
15. R.-D. Kahlke, *The History of the Origin, Evolution and Dispersal of the Late Pleistocene Mammuthus-Coelodonta Faunal Complex in Eurasia (Large Mammals)* (Fenske Companies, Rapid City, SD, 1999).
16. E. A. Vangengeim, E. I. Beljaeva, V. Y. Garutt, E. L. Dmitrieva, V. S. Zazhigin, *Trudy Geol. Inst. Akad. Nauk SSSR* **152**, 92 (1966).
17. G.-f. Zong, Q. Q. Xu, W. Y. Chen, *Vert. PalAsiat.* **23**, 161 (1985).
18. S.-h. Zheng, W.-y. Wu, Y. Li, *Vert. PalAsiat.* **23**, 89 (1985).
19. X. Wang *et al*., *Palaeogeogr. Palaeoclimatol. Palaeoecol.* **254**, 363 (2007).
20. H. R. Rezaei *et al*., *Mol. Phylogenet. Evol.* **54**, 315 (2010).
21. A. Hassanin, A. Ropiquet, *Mol. Phylogenet. Evol.* **33**, 896 (2004).
22. N. K. Verestchagin, *Dokl. Akad. Nauk SSSR* **99**, 455 (1954).
23. R.-D. Kahlke, *Quaternaire Hors-Série* **3**, 21 (2010).
24. P.-O. Antoine, *Mém. Mus. Natl. Hist. Nat.* **188**, 1 (2002).

Acknowledgments: We thank M. Zhao, J. Liu, S.-k. Hou, C.-f. Zhang, W.-q. Feng, F.-q. Shi, S.-l. Wu, and Z.-d. Zhang for their participation in the fieldwork; Z.-d. Qiu for logistical planning and general guidance; E. H. Lindsay for access to collections under his care; Y.-f. Xu for assistance in isotope analysis; W.-l. Shen for illustration; H. W. Thomas for preparation of Zanda fossils; and R.-D. Kahlke for discussion of early records of *Coelodonta*. W. Shifeng provided Global Positioning System coordinates for his paleomagnetic sections, and P. Blisniuk offered useful consultation on fossil localities. Fieldwork was supported by the Chinese National Natural Science Foundation (grant no. 40702004 to Q.L. and grant no. 40730210 to T.D.), Chinese Academy of Sciences (KZCX2-YW-Q09), National Geographic Society (grant no. W22-08 to Q.L.), and NSF (grants EAR-0446699 and EAR-0958704 to X.W., EAR-0444073 and EAR-0958602 to Y.W., and EAR-0438115 to P. DeCelles). Isotope analysis was performed at the Florida State University Stable Isotope Laboratory, supported by NSF (grant EAR-0517806).

Supporting Online Material

www.sciencemag.org/cgi/content/full/333/6047/1285/DC1
SOM Text
Figs. S1 to S13
Tables S1 to S8
References (*25*–*130*)

5 April 2011; accepted 27 July 2011
10.1126/science.1206594